AUSTRIAN JOURNAL OF EARTH SCIENCES
[MITTEILUNGEN DER ÖSTERREICHISCHEN GEOLOGISCHEN GESELLSCHAFT]

AN INTERNATIONAL JOURNAL OF THE AUSTRIAN GEOLOGICAL SOCIETY
VOLUME 97 2004 2005

EDITING: Grasemann Bernhard, Wagreich Michael
PUBLISCHER: Österreichische Geologische Gesellschaft
Neulinggasse 38, A-1031 Wien
TYPESETTER: Irnberger Norbert, www.irnberger.net
Copy-Shop Urban, Bahnstraße 26a, 2130 Mistelbach
PRINTER: Holzhausen Druck & Medien GmbH
Holzhausenplatz 1, 1140 Wien
ISSN 0251-7493

Austrian Journal of Earth Sciences | Volume 97 | 16 - 23 | Vienna | 2005

Indications for activity of the Brenner Normal Fault zone (Tyrol, Austria) from seismological and GPS data

F. REITER[1)*)], W. A. LENHARDT[2)] & R. BRANDNER[1)]

KEYWORDS

focal plane mechanism
Brenner normal fault
fault plane solution
lateral extrusion
active faulting
GPS

[1)] Institute for Geology and Paleontology, University of Innsbruck, Innrain 52, 6020 Innsbruck, Austria

[2)] Seismological Service of Austria, Central Institute for Meteorology and Geodynamics, Hohe Warte 38, 1190 Vienna, Austria

[*)] Corresponding author, franz.reiter@uibk.ac.at

Abstract

For the Brenner Normal Fault (BNF), a ductile and brittle history has to be considered. The ductile part of the BNF is a low-angle, W-dipping mylonite zone which compensated the exhumation of the western Tauern Window during Neogene convergence between the Adriatic and European plates. In addition, the contact between the foot- and hangingwall blocks is marked by a discrete brittle fault which dips moderately to W. The area W of the BNF surface trace and south of the Upper Inn Valley is seismically characterized by low magnitude events. Earthquake epicentres are scattered in a broad zone which extends up to 15 km west of the BNF. Hypocenter depths range between 5 and 18 km. The density of epicentres continuously decreases towards W while the depth of hypocenters increases. Focal plane solutions can be separated into three categories: (1) Strike-slip earthquakes (NE or NW striking faults) indicating N-S shortening; (2) A second group of solutions proves E-W extension, possibly at the BNF; (3) A third group of events was produced by thrust faults, indicating N-S-shortening at different crustal levels. Preliminary data of permanent GPS stations located on both sides of the BNF and in the north Alpine foreland indicate N/NW directed movement of the Alpine stations relative to the foreland in the order of ~1 mm/yr and E-W extension across the BNF in the order of ~0.5 mm/yr. As a model for active crustal movements we suggest (1) N(NW)-directed thrusting of the central Alpine nappe stack and (2) contemporaneous E-W extension which uses the weakness zone of the BNF.

Die Brenner-Abschiebung weist eine duktile und spröde Geschichte auf. Der duktile Abschnitt besteht aus einer flach W-fallenden Mylonitzone, die die Exhumierung des westlichen Tauernfensters während der Neogenen Konvergenz zwischen der Adriatischen und Europäischen Platte kompensierte. Zusätzlich existiert am Kontakt der Liegend- und Hangendeinheiten eine diskrete Sprödstörung, die ebenfalls flach nach W einfällt. Das Gebiet westlich des Ausstrichs der Brennerabschiebung und südlich des Oberinntals ist seismisch durch Ereignisse mit geringer Magnitude charakterisiert. Die Erdbeben-Epizentren sind entlang einer etwa 15 km breiten Zone westlich der Störung verteilt. Erdbeben-Hypozentren befinden sich im Tiefenbereich von 5 bis 18 km. Die Dichte der Epizentren nimmt mit zunehmender Entfernung von der Störung ab, während die Tiefe der Hypozentren zunimmt. Herdflächenlösungen aus dem Untersuchungsgebiet können in drei Gruppen unterteilt werden: (1) Seitenverschiebungsbeben an NE oder NW streichenden Störungen, die N-S-Verkürzung anzeigen; (2) Eine zweite Gruppe von Lösungen weist auf E-W Dehnung hin, die Beben sind wahrscheinlich an der Brenner-Abschiebung angeordnet; (3) Überschiebungsbeben, die N-S Verkürzung in verschiedenen krustalen Stockwerken anzeigen. Vorläufige Daten von permanent-GPS-Stationen beiderseits der Brennerabschiebung und im Alpenvorland, weisen auf eine N bis NW gerichtete Bewegung der alpinen Stationen relativ zum Alpenvorland hin, mit einer Größenordnung von ~1 mm/a, sowie auf eine E-W Dehnung über die Brennerabschiebung von ~ 0.5 mm/a. Als Modell für die aktiven Krustenbewegungen schlagen wir (1) N(NW) gerichtete Überschiebung des alpinen Deckenstapels und (2) gleichzeitige E-W Dehnung an der vorgegebenen Schwächezone der Brenner-Abschiebung vor.

1. Introduction

For some years now Global Positioning Systems (GPS) stations are continuously observing the crustal deformation field on a continental scale. First results of these networks indicate ongoing convergence across the alpine chain of up to several mm per year, driven by a counter clockwise rotation of the Adriatic Plate in respect to stable Europe (Caporali and Martin, 2000; Grenerczy et al., 2000; Nocquet and Calais, 2003). Terrestrial geodetic data from the central Alpine area show active uplift in the order of 1-2 mm per year (Senftl and Exner, 1973; Höggerl, 2001; Schlatter and Marti, 2002).

Geoscientific research increasingly focuses on the state of stress and strain within the alpine chain to depict the internal deformation pattern. Recent studies have shown that the overall NW-SE directed stress field is subjected to major disturbances in the Alps depending on orogen strike (Reinecker and Lenhardt, 1999; Kastrup et al., 2004). The earthquake distribution in the eastern Alps clearly denotes some zones where we should expect differential crustal movements due to surface faulting (Fig. 1). Despite of earthquake and geodetic data indicating that active faults on the surface should be expected, for most alpine areas geomorphologic and gravitational processes heavily superimpose slow crustal movements and reports about outcropping active faults are scarce (e.g. Persaud and Pfiffner, 2004).

We start from a well-investigated fault of Miocene age – the Brenner Normal Fault - and try to prove its recent activity by the means of geological, earthquake and GPS data, which all three should give a consistent image of active orogenic movements. This approach is possible because of an earthquake and permanent-GPS station network close to the investigated area.

2. Tectonic setting

Two styles of deformation are associated with the Brenner Normal Fault (BNF, Fig. 2). The ductile portion of the BNF is a low-angle W-dipping normal fault that compensated the exhumation of the western Tauern Window during Neogene convergence between the Adriatic and European plates. Shear sense indicators within the several 100 m thick mylonite zone indicate top to W movement (Behrmann, 1988; Selverstone, 1988; Fügenschuh et al., 1997). Thermochronological data suggest a Neogene vertical displacement of up to 20 km in the western part of the Tauern Window (Grundmann and Morteani, 1985; Fügenschuh et al., 1997).

In addition to the Brenner mylonite zone, the contact between the foot- and hangingwall blocks is marked by a discrete brittle fault which can be traced from Sterzing to Innsbruck (Fig. 2; Sander et al., 1921; Schmidegg, 1953; Fuchs, 1966; Behrmann, 1988). For this brittle part of the BNF a vertical displacement of 4-5 km after 13 Ma is interpreted from fission track studies (Fügenschuh et al., 1997).

3. Geological field evidence

The brittle Brenner Normal Fault is scarcely exposed and may not be recognized on digital elevation models or in remote sensing due to its moderate dip angle (30-45°), deep seated slope deformation, and rocks with similar rheological behaviour on either side of the fault. In the area SW of Innsbruck further obliteration of topographic features attributed to the brittle BNF is caused by young quaternary deposits and anthropogenic influence (Fig. 2). In an abandoned clay pit south of Innsbruck (Locality “Stefansbrücke”) the brittle BNF was exposed until 2004 (location indicated in Fig. 2). In this outcrop the BNF separates paragneiss of the Ötztal crystalline basement in the hangingwall from quartzphyllites of the Lower Austroalpine in the footwall. Structural investigations revealed that the fault core zone is characterized by an ultracataclasite of several 10s of meters thickness. The fault rock consists of finely crushed crystalline material, newly formed clay minerals and porphyroclasts of former quartz segregations from the quartzphyllite and paragneiss (Figs. 3 A-C). The ultracataclasite foliation dips with 10° to 50° towards SW. Together with the fault surface trace this indicates that the brittle BNF bends from N to NW strike when it approaches the Oberinntal fault zone (Fig. 2). The orientation of elongated porphyroclasts suggests top to W(SW) movement (Fig. 3D). We interpret NW- striking high angle faults as secondary faults to the moderately SW dipping master fault (Fig. 3A, B, D).

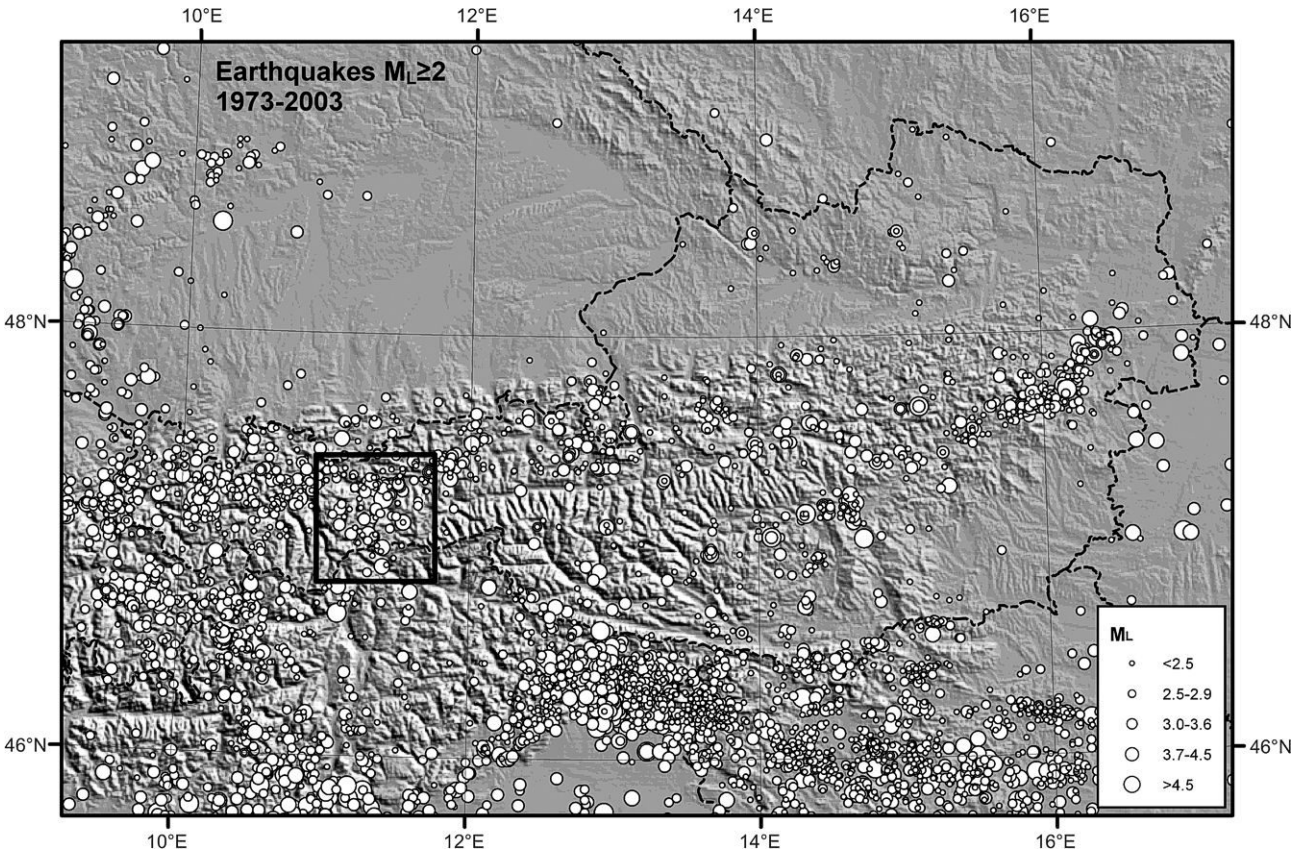

Figure 1: Instrumentally recorded earthquakes in Austria and surrounding regions 1973-2003 and the area investigated (small rectangle). Source: ZAMG, 2004 (Austria), National Earthquake information center http://neic.usgs.gov (outside Austria).

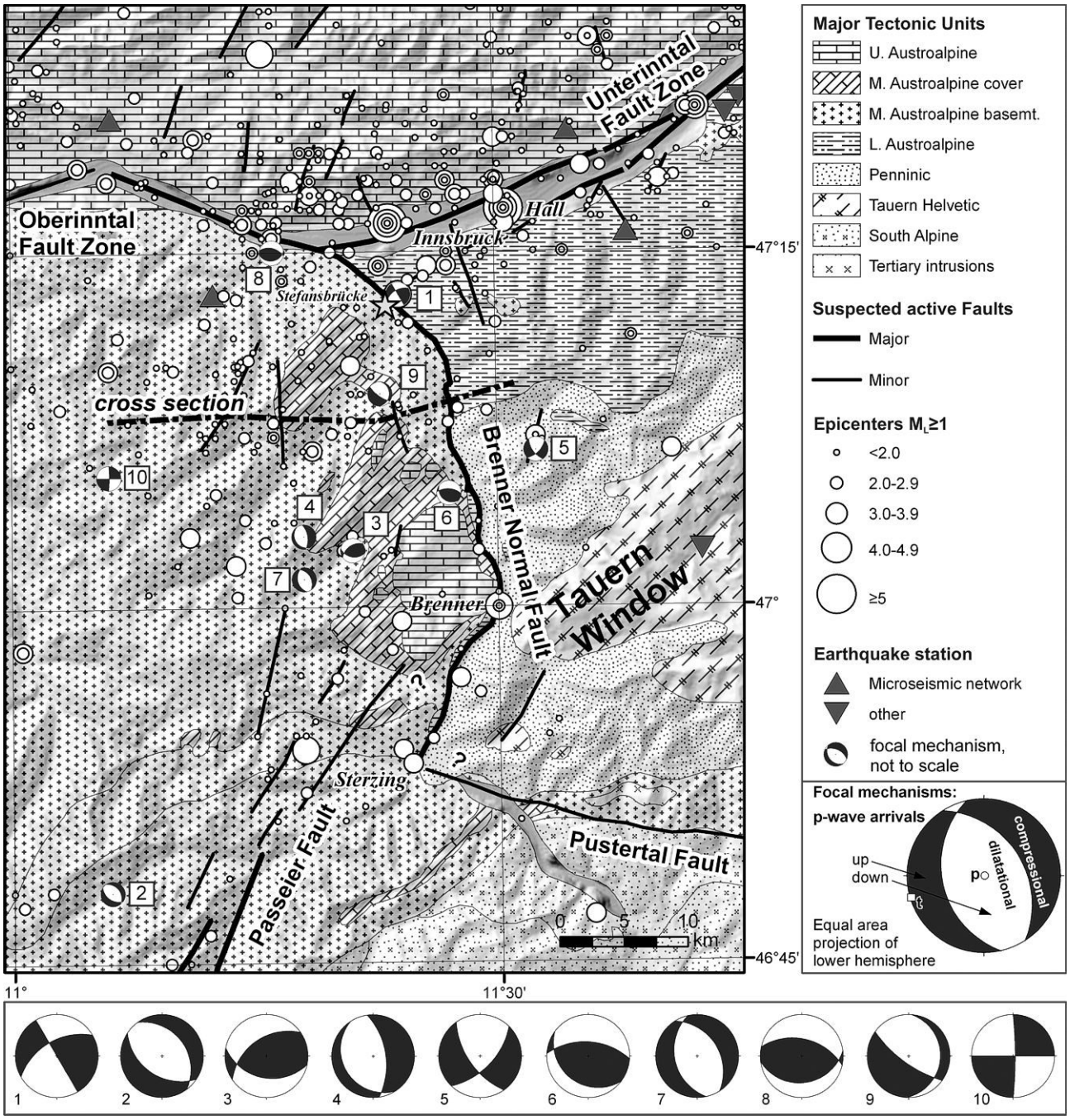

Figure 2: Shaded relief and tectonic map of the western margin of the Tauern Window. The Brenner normal fault separates the Middle and Upper Austroalpine units in the hangingwall (W) from the units of the Tauern Window and Lower Austroalpine in the footwall (E). Earthquake epicenters, focal mechanisms and earthquake stations are also shown (see text). For focal mechanism details see Tab. 1. Tectonic map modified after Brandner, 1980.

4. Earthquake data acquisition and preparation

We used the ZAMG-earthquake catalogue which includes data back to 1541 for this region (ZAMG, 2004). However at the time being a regional historical seismological analysis is missing and not all earthquake data relevant to this study might have been considered (for the completeness of data see Grünthal et al., 1998). Most low-magnitude located events relate to the last 15 years due to the availability of data from the ZAMG microseismic network that consists of four permanent short period digital one-component seismometers (Fig. 2). One of which was converted to a broadband station in 2003. Due to the station geometry not all events with $M_L \leq 3$ may be recorded from the southern part of the investigated area (Fig. 2). Depth estimation errors can reach up to 5 km, especially for weak earthquakes which were recorded by a few stations only. For felt earthquakes instrumentally determined depths were checked and improved by macro-seismic observations.

For the focal mechanism calculation P-wave first onset polarities from the ZAMG earthquake catalogue (ZAMG, 2004) and from the ISC database were used (ISC, 2004). In addition for events 7 and 8 (Tab. 1) we utilized first motion readings and S_H/P amplitude ratios from TRANSALP stations (Alpine deep reflexion seismic

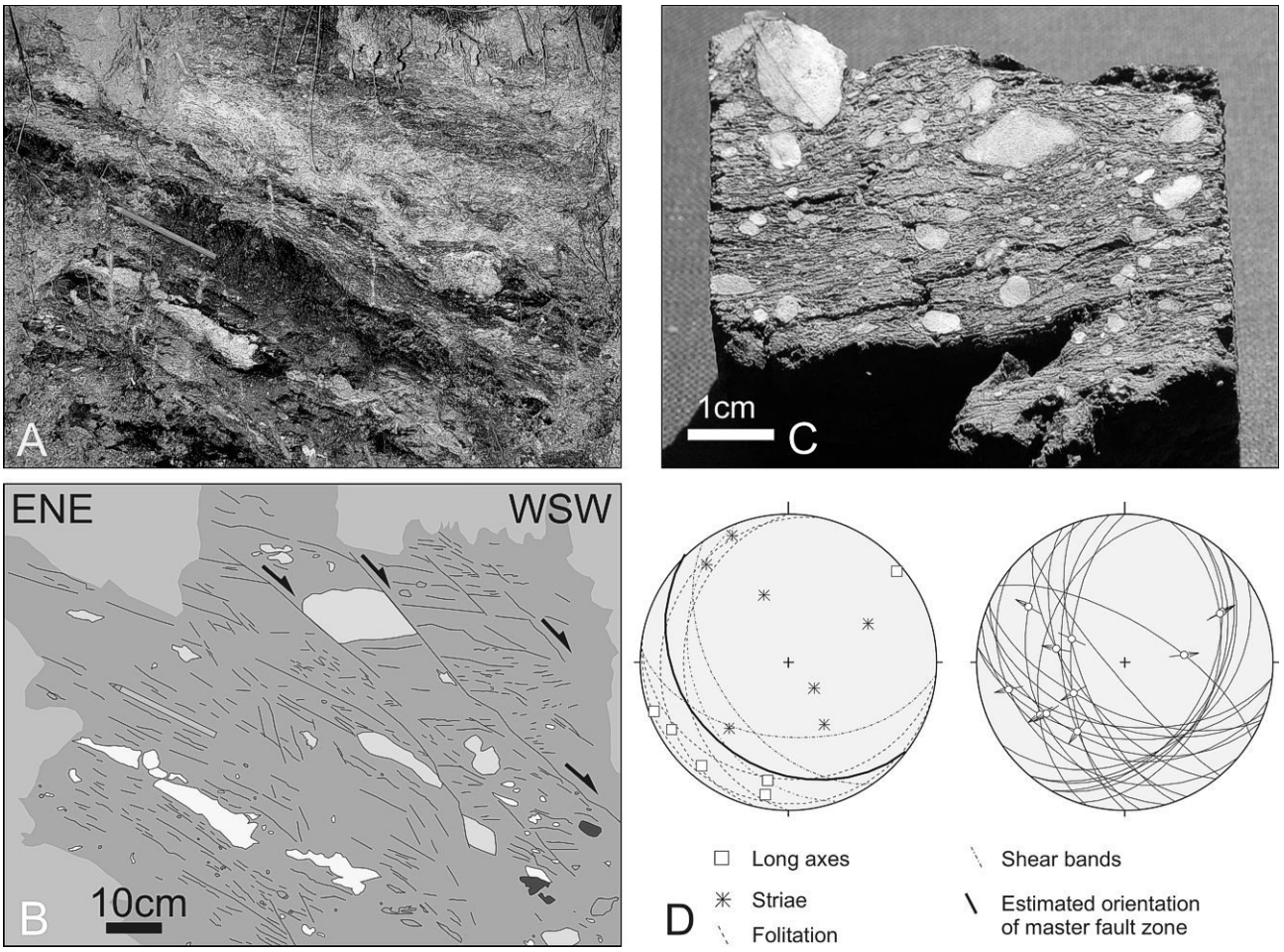

Figure 3: Outcrop data from the Brenner normal fault at the Locality Stefansbrücke (For location see Fig. 2). A, B: Outcrop scale structures in the fault core zone show top to WSW movement. C: Cut hand specimen of the fault rock: Quartz porphyroclasts are embedded in a clay and sheet silicate rich ultracataclasite matrix. D, left: Orientation of porphyroclasts and striae on secondary fault planes show WSW directed and N or S – directed movement. D, right: high-angle normal faults indicate E-W extension.

study). These temporary short-periodic, permanent, digital recording stations were operating continuously during to 1998 (Kraft, 1999). The calculation of take-off angles according to the IASPEI91 crustal model was carried out with FPS 2 for Windows (Reiter and Lenhardt, 2004). For distances below 1° (=111.26 km), which are not stipu-lated by the IASPEI-slow-ness tables, the direct wave path was assumed straight between the hypocentre and the station. Focal mechanisms were then calculated with the program FocMec (Snoke, 2003) and visually checked with FPS 2.

5. Seismicity and focal mechanisms

The area W of the BNF and south of the Upper Inn Valley is seismically

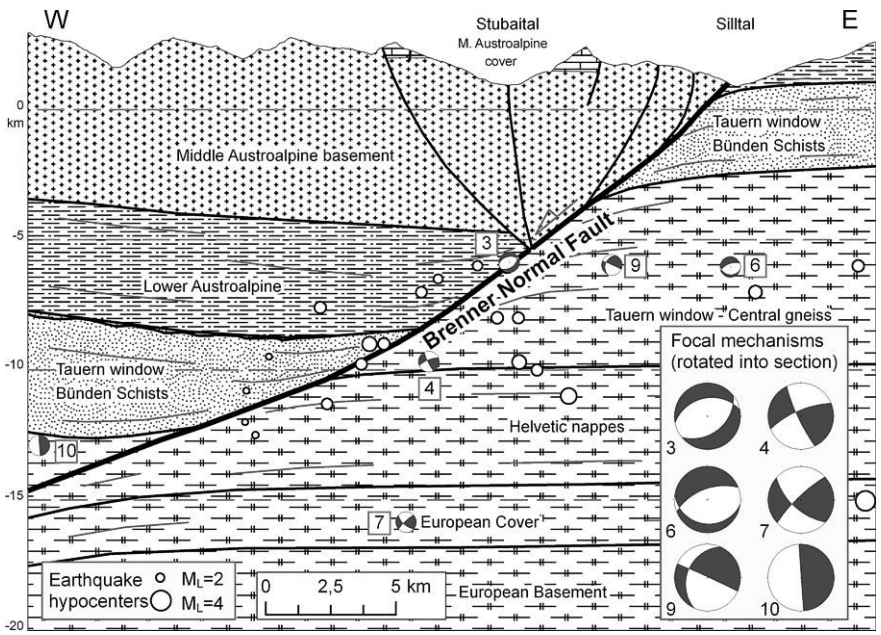

Figure 4: Schematic E-W section across the Brenner Normal Fault, projected earthquake hypocenters and rotated focal mechanisms. Most earthquakes are located between 5 and 20 km W of the Silltal, in a depth between 6 and 17 km. Three focal mechanisms show E-W extension or oblique extension (4, 7, 9), two indicate thrusting (3, 6) and one strike-slip faulting (10).

characterized by low-magnitude events with most earthquakes below M_L=3. The Austrian earthquake catalogue lists 125 events with $M_L \geq 2$, of which 52 were felt. Hypocenter depth information is available for 24 events out of these. The strongest event which may be attributed to the BNF-system occurred in the transition between BNF and Passeier fault W of Sterzing in 1902 with I_0=6 (M_L estimated to 4.2, Fig. 2). Earthquake epicentres in the investigated area are scattered in a broad zone which extends 15 km west of the BNF and with decreasing earthquake density towards W. Figure 4 shows a schematic geologic cross section across the BNF. All depth-located earthquakes W of the Brenner normal fault and S of the Oberinntal Fault were projected into the section. Earthquake hypocentres were shifted

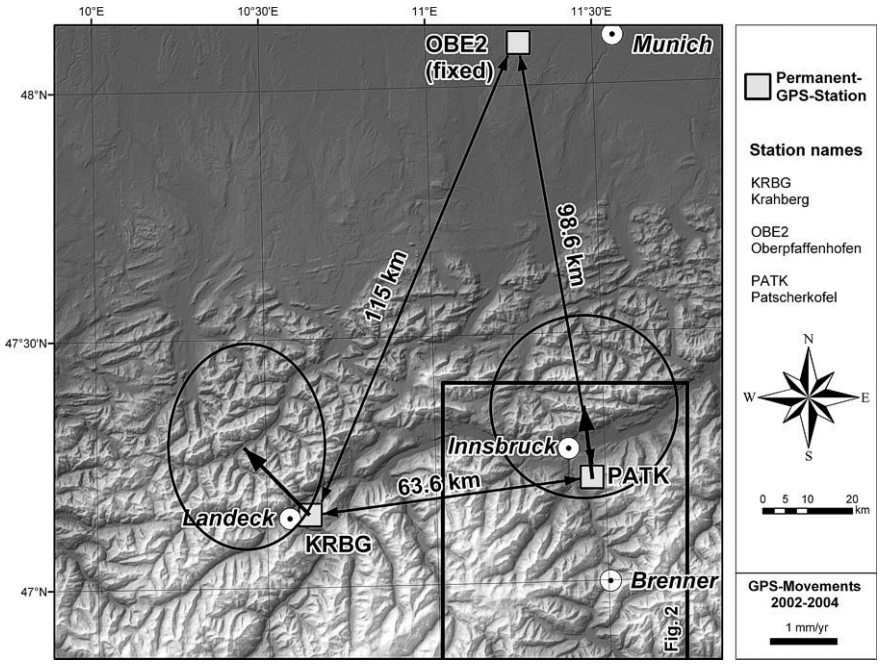

Figure 5: Permanent GPS-Stations of the Austrian GPS network used for calculating distance/time plots. Movement vectors and 95% error ellipses for Stations KRBG and PATK relative to Station OBE2 are plotted. See Diagrams (Figs. 6, 7) and text for details.

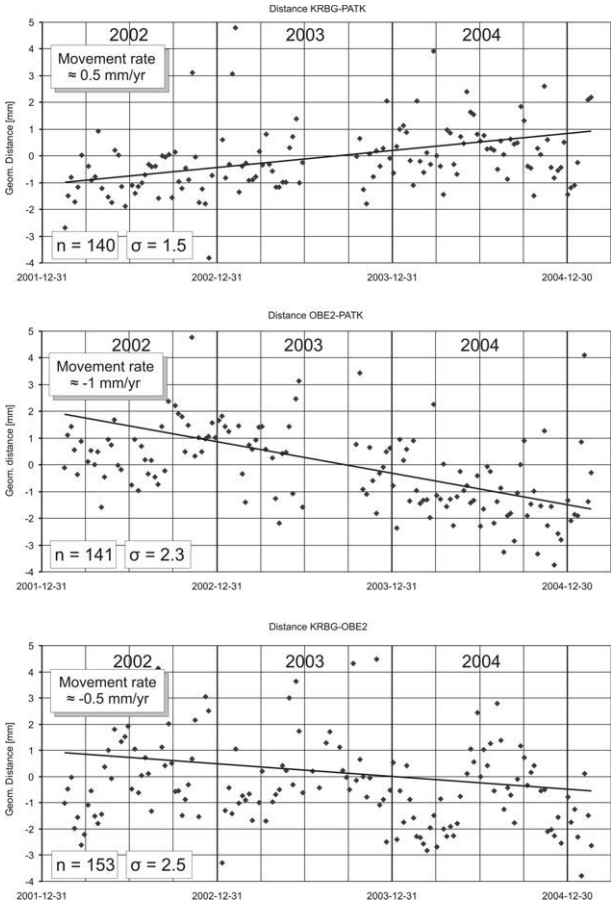

Figure 6: Geometric distance between KRBG-PATK, OBE2-PATK and KRBG-OBE2 for the period 2001-2004. Distances were calculated from Austrian reference weekly solutions calculated by the OLG datacenter in Graz.

horizontally in north or south direction into the section plane. The depth of earthquake hypocenters ranges between ~ 5 and 18 km and increases towards W. All events seem to be located in the footwall or directly on the BNF.

Due to the observed moderate seismicity and its low magnitude events, no moment tensor inversions are available for the investigated area by now, because more records from seismic stations are needed for such a task. A kinematic interpretation of these earthquakes has been carried out by the focal plane solution method, instead. The results of the calculations are shown in Tab. 1, in chronological order, on the tectonic map (Fig. 2) and in a schematic E-W section (Fig. 4). The dihedra diagrams used in Figs. 2 and 4 ("beachballs") are lower hemisphere projections showing the 2 nodal planes as great circles. Dihedra where p-wave first motions arrive compressively (first motion up) plot are coloured in grey. These are the distensive dihedra in terms of stress, i.e. where minimum principal stress is located. The positions of minimum (t) and maximum principal stress axes (p) are shown in an example diagram in Fig. 2, lower right.

Events 1, 5 and 10 (numbers according to Tab. 1, Figs. 2 and 4) were generated by strike-slip fault activity. Earthquakes 1 and 5 occurred in the footwall of the BNF and probably indicate sinistral strike-slip faulting at NE striking subvertical faults of the units bordering the Tauern Window to the north. Earthquakes 2, 4, 7 and 9 are indicators of normal or oblique normal faulting. All of them are located W of the BNF surface trace and can be attributed to E-W extension on a moderately W(SW)-dipping fault with a seismic zone between 5 and 16 km. Events 3, 6 and 8 were generated by thrust faulting. We interpret them as indicators for active N-S shortening which occurs contemporaneously with E-W extension. Event 8 is located close to the Oberinntal fault and could prove N-directed thrusting of the

Austroalpine unit W of the BNF. Events 3 and 6 are situated W of the BNF surface trace but might be located in the BNF footwall units (Tauern window/Helvetic nappes), where N-S shortening also causes active thrust ctivity, too.

6. GPS-Data

GPS-Stations of the Austrian Academy of Science and of the EUREF permanent network exist on both sides of the fault (stations Patscherkofel – "PATK" near Innsbruck and Krahberg – "KRBG" next to Landeck) and in the Alpine foreland (station Oberpfaffenhofen – "OBE2" near Munich, Fig. 5). Reliable time series these three stations are available since the beginning of 2002. Austrian GPS reference frame weekly solutions from the OLG-data centre (Observatory Lustbühel) in Graz were used (http://gps.iwf.oeaw.ac.at/olgdc1.htm). Seasonal variations are very common to EUREF data (cf. Fig. 6, base line KRBG-OBE2). In order to minimize the seasonal influence on the short data record available, we have chosen a time span of exact 3 years for evaluation (Feb. 2002-Feb. 2005). For all GPS data linear regression was calculated by the least squares method.

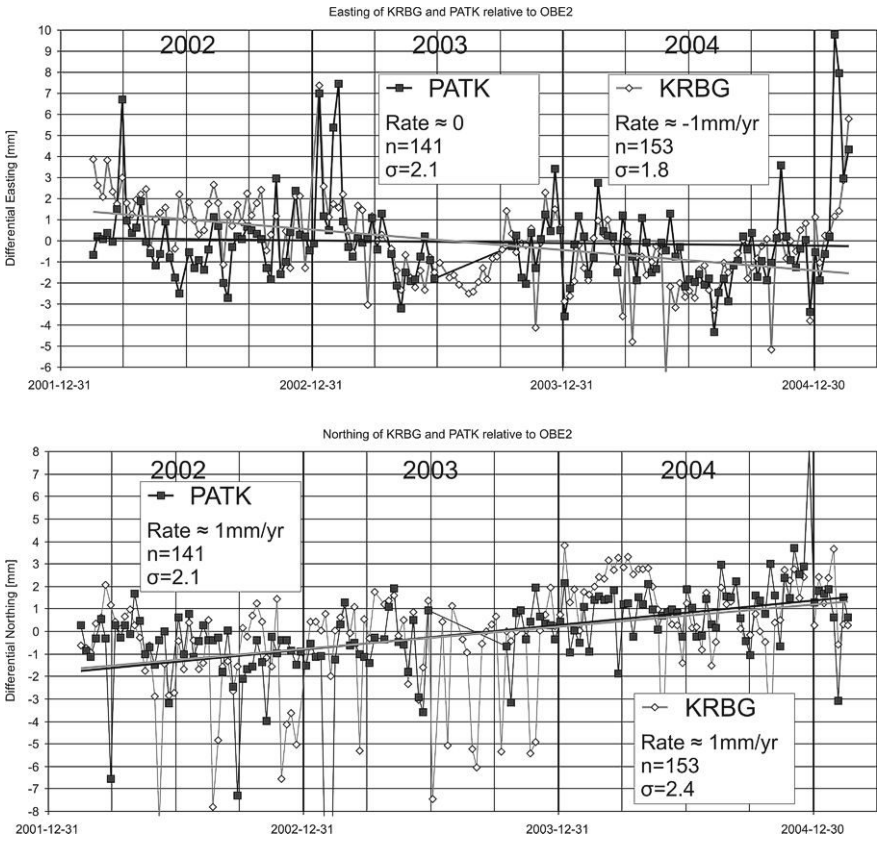

Figure 7: Differential East and North values of Stations KRBG and PATK relative to a fixed station OBE2 for the period 2002-2004. The error ellipses are drawn for 95% confidence (length of half axes equals 1.96*σ). For locations see Fig. 5.

The results of the calculations are shown in Figs 5-7. In Fig. 6 we have calculated baselines (the geometric distance) between the three stations. While the distance of stations KRBG-PATK increases slightly, it decreases between stations KRBG-OBE2 and PATK-OBE2. Due to the slow movement rates and the short observation period, not all results are statistically significant, yet. In Fig. 7 we have fixed Station OBE2 and calculated the E and N directed components of motion for the stations PATK and KRBG, which are located on either sides of the BNF. The movement rates with corresponding error ellipses are shown in Fig. 5. While station KRBG moves towards W, station PATK is almost stable in E-W position in respect to station OBE2. Both stations move at approximately the same rate towards north. As above, the results have to be handled with care due to the low statistical significance, however. Since both alpine stations PATK and KRBG are located on summits of mountains that are built of crystalline basements (gneiss, schist, phyllite), we can not entirely exclude the role of mass movements as the cause for NW directed movements. Due to the very slow movement rates which range between 0.5 and 1 mm/yr, we favour the hypothesis of active crustal movements.

7. Discussion of results and kinematic interpretation

We explain the broad scattering of epicentres towards the west of the BNF and the increasing hypocentral depth from east to west by a moderately W-dipping active fault. This hypothesis is further supported by E-W extensional fault plane solutions. If the GPS data reflect crustal movements, the increasing distance between the stations on either side of the fault would confirm the

No	UTC	Lat	Lon	z	M_L	Plane A	Plane B	P	B	T	n(P)	n(S_H/P)
1	26.02.1984 01:35	47,22	11,40	11	4,4	240/60	150/90	199/21	330/60	101/21	22	
2	02.05.1984 10:28	46,80	11,10	8	3,6	324/41	124/51	340/79	133/10	223/05	15	
3	12.07.1990 09:14	47,04	11,35	6	2,7	235/54	101/46	346/04	254/25	086/65	10	
4	20.08.1990 13:33	47,05	11,30	10	3,6	352/65	147/27	283/68	167/10	073/19	17	
5	17.07.1996 00:54	47,11	11,54	17	3,9	044/66	145/66	004/35	184/55	275/00	13	
6	14.09.1997 15:46	47,08	11,45	6	2,5	274/61	126/33	016/14	282/15	149/69	11	
7	29.08.1998 06:27	47,02	11,30	16	2,8	347/45	148/47	342/80	157/10	247/01	23	9
8	30.09.1998 05:53	47,25	11,27	7	3,0	082/36	273/56	004/10	096/10	230/76	23	11
9	07.08.2000 21:43	47,15	11,38	6	2,5	004/25	036/76	011/54	132/20	233/28	9	
10	04.11.2004 19:11	47,09	11,10	13	3,1	000/86	000/90	315/03	090/86	225/03	21	

Table 1: Numerical results of focal mechanism calculations. Data contained in the table are the universal time coordinated (UTC), the geographical coordinates of the epicenter (lat, lon) and the local magnitude (M_L). For the nodal planes (Plane A, Plane B) strike and dip is given, for P-, B- and T-axes azimuth and plunge. n(P) denotes the number of p-wave first motions and n(S_H/P) the number of S_H/P amplitude ratios used. For location see Figs 2 and 3.

observed earthquakes. Active E-W extension is accompanied by N(NW)-S(SE) directed shortening as indicated by thrust and strike-slip events. Concluded from hypocenter depth, the thrust events are probably located within the alpine nappe stack. Strike-slip events seem to occur in both the foot- and hangingwall blocks of the BNF and compensate differential N/NW directed movements of crustal segments.

If we discuss the results in a regional context, they only partly confirm the model of lateral extrusion by Ratschbacher et al., 1991. This model explains Miocene alpine kinematics - contemporaneous shortening normal to and extension parallel to the orogen - with sets of conjugate sinistral and dextral strike-slip faults bounding eastward moving ("extruding") crustal wedges. According to Ratschbacher et al., 1991, the main driving forces for the extrusion would be a N-directed movement of the Adriatic plate ("indenter") and an unconfined eastern boundary of the alpine nappe stack towards the Pannonian basin. In contrast to Rosenberg et al., 2004, who assumed NNE directed movement of the Miocene Adriatic indenter, we expect active N/NW directed movement direction at the northern tip of the Adriatic microplate, which is in line with the counterclockwise rotation of the plate as described by Nocquet and Calais, 2003. We interpret the heterogeneous kinematic pattern observed as the result of a complex stress/strain distribution in the front of the indenter tip. Active indentation causes (1) overall N(NW)-directed thrusting of the entire Alpine nappe stack, accompanied by conjugate NE and NW directed strike-slip faulting, (2) E-W extension at the tip of the indenter which utilizes the weakness zone of the BNF and (3) possibly ongoing folding and uplift of the Tauern dome (Senftl and Exner, 1973; Höggerl, 2001).

According to the lateral extrusion model, sinistral movement on the Unterinntal fault should be kinematically linked to the extension on the BNF. Some of the earthquakes investigated indicate NE directed sinistral activity in the footwall of the BNF and north of the Tauern window. On the other hand, up to now no reliable focal mechanisms are available for the Inntal fault zone which should be a major sinistral bounding element in the extrusion model. Investigations of the Inntal fault zone revealed, that at least a part of the earthquakes observed are N- or S-directed thrusts/reverse faults, probably inverting graben structures in the European plate (Reiter et al., 2003). From the area east of the Tauern window evidence for E-directed crustal movements for the area north of the Vienna Basin Transfer Fault relative to stable Europe comes from permanent-GPS (e.g. Grenerczy et al., 2000) and earthquake data (Hinsch & Decker, 2003).

Apart from the extrusion model, the phenomenon of active orogen-parallel extension is not unique to the Brenner Normal Fault. Earthquakes at the eastern border of the Tauern window, east of the surface trace of the E-dipping Katschberg fault zone also show E-W extensional focal mechanisms (e. g. earthquake of 2003-08-25, moment tensor solution available online: SED, 2004). Orogen-parallel extension in the Engadine Alps of eastern Switzerland has been reported by Kastrup et al., 2004 and can also be observed in the southern Ortles massif (Italian Eastern Alps) where several earthquakes with ENE-WSW extensional focal mechanisms occurred in the recent past (earthquakes of the Bormio region from 1999 until 2002, moment tensor solutions: SED, 2004).

8. Conclusion

Earthquake and GPS data support that the Brenner Normal Fault is still active or re-activated. The geometry of active movements at the western border of the Tauern Window resembles the Miocene fault pattern, even if the movement of the Adriatic microplate might be different today. GPS results show, that the movement rates across the BNF zone and probably also across the Oberinntal fault zone are very small, in the order of 0.5 to 1 mm/a (cf. Fig. 5). Longer GPS observation periods and additional stations within the region of the western Tauern window will help to further refine the pattern of active crustal movements in the future.

Acknowledgements

We would like to thank Elena Cristea (OLG Data Centre) for her support in GPS data acquisition and computation, Toni Kraft (Bavarian Seismological Centre) for supporting TRANSALP seismological data and Kurt Decker (University of Vienna), Hugo Ortner (University of Innsbruck) and Jochen Braunmiller (Swiss Seismological Survey) for fruitful discussions. We are grateful to Georg Gangl and Ralph Hinsch for their constructive and helpful reviews and to Jan Behrmann for his useful comments.

References

Behrmann, J.H., 1988. Crustal-scale extension in a convergent orogen: the Sterzing-Steinach mylonite zone in the Eastern Alps. Geodinamica Acta (Paris), 2, 63-73.

Brandner, R., 1980. Tektonische Übersichtskarte von Tirol 1:600.000. Universitätsverlag Wagner, Innsbruck.

Caporali, A. and Martin, S., 2000. First results from GPS measurements on present day alpine kinematics. Journal of Geodynamics, 30, 275-283.

Fuchs, A., 1966. Geologie der Europabrücke. Felsmechanik und Ingenieurgeologie, IV, 317-331.

Fügenschuh, B., Seward, D. and Mancktelow, N.S., 1997. Exhumation in a convergent orogen: the western Tauern window. Terra Nova, 9, 213-217.

Grenerczy, G., Kenyeres, A. and Fejes, I., 2000. Present crustal movement and strain distribution in Central Europe inferred from GPS measurements. Journal of Geophysical Research-Solid Earth, 105, B9, 21835-21846.

Grundmann, G. and Morteani, G., 1985. The young uplift and thermal history of the Central Eastern Alps (Austria, Italy), evidence from apatite fission track ages. Jahrbuch der Geologischen Bundesanstalt, 128, 197-216.

Grünthal, G., Mayer-Rosa, D. and Lenhardt, W. A., 1998. Abschätzung der Erdbebengefährdung für die D-A-CH-Staaten - Deutschland, Österreich, Schweiz. Bautechnik, 75, 19-33.

Höggerl, N., 2001. Bestimmung von rezenten Höhenänderungen durch wiederholte geodätische Messungen. In: C. Hammerl, W.A. Lenhardt, R. Steinacker and P. Steinhauser (Editors), Die Zentralanstalt für Meteorologie und Geodynamik 1851-2001. Leykam, Graz, pp. 630-644.

ISC, 2004. On-line Bulletin. http://www.isc.ac.uk/Bulletin, International Seismological Centre, Thatcham, United Kingdom.

Kastrup, U., Zoback, M. L., Deichmann, N., Evans, K. F., Giardini, D. and Michael, A. J., 2004. Stress Field Variations in the Swiss Alps and the Northern Alpine Foreland Derived from Inversion of Fault Plane Solutions. Journal of Geophysical Research, 109, B01402, 1-22.

Kraft, T., 1999. Die Seismizität der nördlichen Ostalpen und die Herdmechanik ausgewählter Erdbeben. MSc Thesis, Ludwig-Maximilians-Universität, München, 115 pp.

Nocquet, J.-M. and Calais, E., 2003. Crustal velocity field of western Europe from permanent GPS array solutions, 1996-2001. Geophysical Journal International, 154, 72-88.

Persaud, M. and Pfiffner, O. A., 2004. Active deformation in the eastern Swiss Alps: post-glacial faults, seismicity and surface uplift. Tectonophysics, 385, 59-84.

Ratschbacher, L., Frisch, W., Linzer, H.-G. and Merle, O., 1991. Lateral extrusion in the Eastern Alps, Part 2: Structural Analysis. Tectonics, 10, 257-271.

Reinecker, J. and Lenhardt, W. A., 1999. Present-day stress field and deformation in eastern Austria. Geologische Rundschau, 88, 532-550.

Reiter, F. and Lenhardt, W. A., 2004. FPS2 for Windows. Unpublished computer program for handling and visualization of fault plane solution data.

Reiter, F., Ortner, H. and Brandner, R., 2003. Seismically active Inntal fault zone: inverted European rift structures control upper plate deformation. Mem. Soc. Geol. Ital., 54, 233-234.

Rosenberg, C. L., Brun, J.-P. and Gapais, D., 2004. Indentation model of the Eastern Alps and the origin of the Tauern Window. Geology 32(11), 997-1000.

Sander, B., Ampferer, O. and Spengler, E., 1921. Zur Geologie der Zentralalpen. Jahrbuch der Geologischen Bundesanstalt, 71, 173-224.

Schlatter, A. and Marti, U., 2002. Neues Landeshöhennetz der Schweiz LHN95. Mensurat. Photogramm. Genie Rural, 1, 13-17.

Schmidegg, O., 1953. Die Silltalstörung und das Tonvorkommen bei der Stefansbrücke. Verhandlungen der Geologischen Bundesanstalt, 1953, 135-138.

SED, 2004. Regional Moment Tensor Catalog. Swiss Seismological Service. http://www.seismo.ethz.ch/mt/.

Selverstone, J., 1988. Evidence for east-west crustal extension in the eastern Alps: implications for the unroofing history of the Tauern Window. Tectonics, 7, 87-105.

Senftl, E. and Exner, C., 1973. Rezente Hebung der Hohen Tauern und geologische Interpretation. Verhandlungen der Geologischen Bundesanstalt, 1973, 209-234.

Snoke, J.A., 2003. FOCMEC: FOcal MEChanism determinations. In: W.H.K. Lee, H. Kanamori, P.C. Jennings and C. Kisslinger (Editors), International Handbook of Earthquake and Engineering Seismology. International Geophysics Series. Academic Press, Amsterdam, pp. 1629-1630.

ZAMG, 2004. Austrian earthquake catalogue. Unpublished computer file. Seismological Service of Austria, Central Institute for Meteorology and Geodynamics, Vienna.

Received: 28. January 2005
Accepted: 23. May 2005

F. REITER[1)*], W. A. LENHARDT[2)] & R. BRANDNER[1)]

[1)] Institute for Geology and Paleontology, University of Innsbruck, Innrain 52, 6020 Innsbruck, Austria

[2)] Seismological Service of Austria, Central Institute for Meteorology and Geodynamics, Hohe Warte 38, 1190 Vienna, Austria

[*)] Corresponding author, franz.reiter@uibk.ac.at